

# On-orbit Spatial Resolution Estimation of CBERS-1 CCD Imaging System

Kamel Bensebaa

*Doctorate Student in applied computation at  
National Institute for Space Research (INPE)  
camel@dpi.inpe.br*

Gerald Jean Francis Banon

*Image processing Department - INPE  
banon@dpi.inpe.br*

Leila Maria Garcia Fonseca

*Image processing Department - INPE  
leila@dpi.inpe.br*

## Abstract

*The first China-Brazil Earth Resources Satellite (CBERS-1) launched in 1999 was designed to capture high-resolution images using a set of sophisticated sensors: Wide Field Imager (WFI), High Resolution CCD Camera (CCD) and Infrared Multispectral Scanner (IR-MSS) imaging systems. The performance of these sensors can be evaluated through PSF measurement that enables an objective assessment of the spatial resolution. This work describes an original approach to estimate on-orbit CBERS1-CCD spatial resolution using images of a simulated black squared target in the Gobi desert.*

## 1. Introduction

The amount of satellite imagery has widely increased with new-sophisticated imaging systems onboard new generation satellites. These systems have provided high quality data and have allowed a more accurate understanding of the phenomena on the ground.

Among this new generation of satellites, the CBERS-1 (China-Brazil Earth Resources Satellite), jointly developed by Brazil and China, was launched on October 14th 1999. The sensors on-board CBERS1 (CCD, IRMSS and WFI) combine features that are especially designed to cover the broad range of space and time scales involved in monitoring and preservation of the ecosystem. CBERS-1 is the first of four earth observation satellites foreseen to be developed within the China-Brazil spatial cooperation program.

The imaging systems are designed to minimize the blurring of the scene radiance field during image acquisition. The residual blurring is attributable to optical diffraction, focal-plane integration by the detectors, analog signal processing, and other physical processes. The blurring effect is related to the shape of the Point Spread

Function (PSF) or in the frequency domain to the shape of the Modulation Transfer Function (MTF). PSF or MTF is a standard measure of an imaging system performance and it enables an objective assessment of its spatial resolution [5][11][14].

Before launching, band 4 (0,77 - 0,89  $\mu\text{m}$ ) of the CBERS1-CCD camera presented a myopia distortion due to a problem in the camera montage. At this time, some image simulation tests were performed in order to check the possibility of the resolution correction through restoration technique [4].

Storey [13] has provided a methodology to measure the Landsat-TM on-orbit spatial response using ground target such as bridges. Choi [6] has used as targets airport runway and a tarp placed on the ground for on-orbit Modulation Transfer Function (MTF) measurement of IKONOS Satellite sensor.

In general, the spatial response is determined in terms of the Point Spread Function or Modulation Transfer Function through parameter known as EIFOV (Effective Instantaneous Field of View) [3]. This parameter is defined as a function of the MTF and it enables a comparison between different sensors with similar nominal spatial resolution.

This paper describes an original approach to estimate the spatial resolution of the CBERS-1 CCD camera. The CCD spatial response is modeled as a 2D Gaussian function which is characterized by two parameters: one in along-track direction and another one in across-track direction. The EIFOV's are then derived from these parameters.

## 2. CBERS-1 overview

The first China & Brasil Earth Resources Satellite (CBERS-1) was launched on 14 October 1999 by the Chinese launcher Long-March 4B, from the Tayuan Launch Center, in the Popular Republic of China. The CBERS-1 payload consists of three instruments called:

CCD (Charge Coupled Device) camera, IRMSS (Infrared MSS) and WFI (Wide Field Imager), which can make optical observation for global area and transmit remotely sensed data to ground receiving stations [10]. The high-resolution CCD Camera has 4 spectral bands from visible light to near infrared and one panchromatic band (See Table 1). It takes the earth ground scenes by pushbroom scanning, on 778 km sun-synchronous orbit, and provides images of 113 km wide strips with sampling rate of 20 meters at nadir [1].

The signal acquisition operates in two channels called CCD1 and CCD2. The first one generates images corresponding to B2, B3 and B4 while the second generates images corresponding to the bands B1, B3 and B5. In each channel, three CCD chips per band were glued to generate about 6000 pixels per row [12].

**Table1. Spectral bands of CCD sensor**

| Spectral Bands | Band Number | Wavelength                |
|----------------|-------------|---------------------------|
| Blue           | 1           | 0,45 - 0,52 $\mu\text{m}$ |
| Green          | 2           | 0,52 - 0,59 $\mu\text{m}$ |
| Red            | 3           | 0,63 - 0,69 $\mu\text{m}$ |
| Near-Infrared  | 4           | 0,77 - 0,89 $\mu\text{m}$ |
| Pan.           | 5           | 0,51 - 0,73 $\mu\text{m}$ |

### 3. PSF estimation methodology

Basically, there exist three ways to determinate the PSF. The first one uses target images. The targets must have well-defined shape and size as airport runway, bridges, etc or artificial target. The second method utilizes images acquired by higher resolution sensor, which are compared with the image under study. Finally, the third one uses the system design specifications and the system analytic model [7][8].

The first two approaches have the advantage of estimating the imaging system PSF by using only the image acquired by the system. In this work, we have opted for the first approach due its simplicity. Besides, we have used image of a squared black target placed on the ground.

#### 3.1. Target images

The target used in this project consists of a black tarp placed in the Gobi desert, creating contrast with the desert. The Dunhuang test site of Gobi desert is situated at about 35 Km west of Dunhuang city in Gansu Province. It corresponds to the alluvial fan of the Dang River, which has frequently moved. Its dimensions are about 30 km from south to north and 40 km from east to west. The black tarp taken as a target is a square shape 60m x 60m in

size with opposite edges nearly aligned with the along-track direction (see Figure.1).

### 3.2. Data preparation

Through the CBERS-1 imaging system, the image of the black tarp was acquired on September 4, 2000. The original image, cloud free was a candidate for along-track and across-track PSF estimation. Figure 2 shows the band 3 with the black target in the image center. In order to facilitate the visualization the image was zoomed up. In this work, only image bands B2, B3, and B4 were processed.



**Figure 1. Setting up of black tarp in Gobi desert**

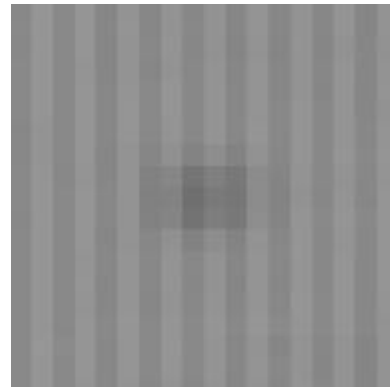


**Figure 2. Original target band 3 image**

#### 3.3. Destriping

The original images acquired by CBERS-1 system have a striping effect as shown on Figure 2. Odd columns are brighter than even columns. This is due to the non-uniform detector gains, since each detector is responsible for one column in the images. The processing procedure to remove the striping effect is described below [2].

Let  $E$  be an image rectangular domain with an even number of columns, and let  $E_e$  and  $E_o$  be the sets of pixel positions belonging, respectively, to the even and odd columns of  $E$ .

Let  $f$  be the original CBERS-1 image. The destriped image  $g$  is given by:

$$g(x) = \begin{cases} a_e f(x) + b_e & \text{if } x \in E_e \\ a_o f(x) + b_o & \text{if } x \in E_o \end{cases}, \quad x \in E$$

where  $a_e = \frac{s}{s_e}$ ,  $a_o = \frac{s}{s_o}$ ,  $b_e = m - a_e \cdot m_e$  and

$$b_o = m - a_o \cdot m_o,$$

where  $m_e$  and  $m_o$  are the means of the original image restricted, respectively, to  $E_e$  and  $E_o$ .  $s_e$  and  $s_o$  are the standard deviations of the original image restricted, respectively, to  $E_e$  and  $E_o$  and  $m = (m_e + m_o)/2$  and  $s = (s_e + s_o)/2$ .

Figure 3 shows the destriped image. One can observe that the striping effect has been completely eliminated without removing the target information.

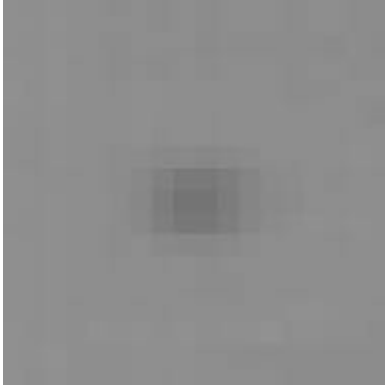


Figure 3: Target band 3 image after destriping

### 3.4. Digital target model

Let  $\mathbf{Z}$  be the set of integer numbers and let  $\mathbf{Z}^2$  be the Cartesian product of  $\mathbf{Z}$  by itself.

Let  $x \in \mathbf{Z}$ , we denote by  $\underline{x}$  the pair  $(x, x)$  of  $\mathbf{Z}^2$ . For example  $\underline{10}$  stands for pair  $(10, 10)$ .

Let  $F$  be a finite square of  $\mathbf{Z}^2$  with an odd number of lines and columns representing the digital scene domain in which the distance between two consecutive horizontal or vertical points is one meter for convenience.

Let  $u$  be the center point of  $F$ . Based on radiometric or geometric features of the target placed in Gobi desert, the digital target model is the function  $f$  on  $F$  given by

$$f_t(x) = \begin{cases} t & \text{if } x \in [u - \underline{30}, u + \underline{30}], x \in F \\ s & \text{otherwise} \end{cases}$$

where  $s$  and  $t$  are, respectively, the background (desert) and target radiometry values, and  $[a, b]$  is the rectangle of  $\mathbf{Z}^2$  having  $a$  as lower left corner and  $b$  as upper right corner. We observe that the digital target model is centered at  $u$  and have size  $60\text{m} \times 60\text{m}$  (see Figure 4).

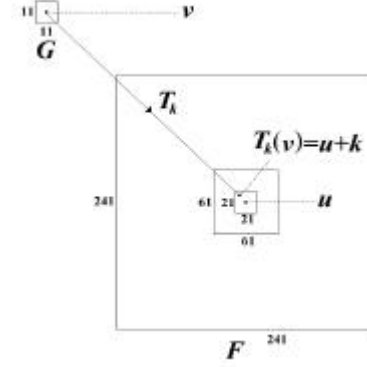


Figure 4: Digital target model

### 3.5. System point spread function

The overall CBERS-1 CCD on-orbit PSF is composed of the PSF's of each sub-system: optics, detector, electronics, instability, etc. In this work the system point spread function is modeled as a 2D Gaussian function  $h_{\delta_1, \delta_2}$  on  $F$ , centered at  $u$ , that is,

$$h_{s_1, s_2}(x_1, x_2) = \frac{1}{2\pi s_1 s_2} e^{-\left(\frac{(x_1 - u)^2}{2s_1^2} + \frac{(x_2 - u)^2}{2s_2^2}\right)}$$

$$(x_1, x_2) \in F.$$

### 3.6. Target image simulation

Let  $G$  be a finite square of  $\mathbf{Z}^2$  with an odd number of rows and columns, representing the target image domain, let  $v$  be the center point of  $G$  and let  $T$  be a geometric transformation from  $G$  to  $F$  given by

$$T_k(y) = 20 \cdot (y - v) + u + k, \quad y \in G,$$

where  $k \in \mathbf{Z}^2$ .

The transformation  $T$  is the target geometric model for the imaging system, where the value equal to 20 represents the distance (in meters) between two consecutive horizontal or vertical pixel positions (sampling rate). The number  $k$  defines how far the transformation of the target image domain center  $v$  is from the digital scene domain center  $u$  (see Figure 4). By assuming that the imaging system is linear, the simulated target image is  $(f_t * h_{s_1, s_2}) \circ T_k$ , where  $*$  is the (circular) convolution

product ( $u$  is being chosen as the origin) on  $F$ , and  $\circ$  is the mapping composition. By composition definition, we observe that the simulated target image is a function on  $G$ .

### 3.7. PSF estimation

Let  $g$  be the target image defined on  $G$ , such that  $g(v)$  has the lowest (recall that the target is black) value among all the pixel values of  $g$ . The PSF estimation consists of finding  $\mathbf{s}_1$  and  $\mathbf{s}_2$  such that  $g$  and  $(f_t * h_{\mathbf{s}_1, \mathbf{s}_2}) \circ T_k$  best fits under the root mean square criteria. Let  $\text{RMS}(f_r, g)$  be the real number given by

$$\text{RMS}(f_t, g) = \left( \sum_{y \in G} ((f_t * h_{\delta_1, \delta_2})(T_k(y)) - g(y))^2 \right)^{1/2}$$

The estimation procedure is a two-steps procedure. At the first step,  $t=g(v)$  and we look for  $k$ ,  $\mathbf{s}_1$  and  $\mathbf{s}_2$  which minimizes  $\text{RMS}(f_r, g)$ .

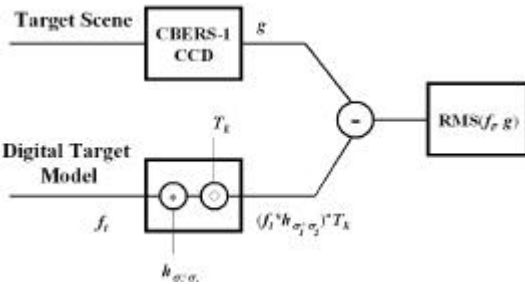


Figure 5. Block diagram of PSF estimation

Because  $g(v)$  is the lowest value among the pixel values of  $g$ , the domain of  $k$  reduces to  $[-10, 10]$  of  $\mathbf{Z}^2$ . At the second step, we use the previous optimum  $k=(k_1, k_2)$  and look for  $t$ ,  $\mathbf{s}_1$  and  $\mathbf{s}_2$  which minimizes  $\text{RMS}(f_t, g)$ . Table 2 shows the estimation results. Figure 6 and Figure 7 show the along-track and across-track fitting between original data and simulated data for band 3.

The desert radiometry  $s$  was estimated by averaging surrounding desert pixel values. In the above estimation, we have used  $F=[1, 241]$ ,  $u=121$ ,  $G=[1, 11]$ ,  $v=6$  and target radiometry value was considered within an interval of  $\mathbf{Z}$  such that  $10.t \in [10.g(v) - 20, 10.g(v) + 20] \subset \mathbf{Z}$ .

Finally, the optimum values of  $\mathbf{s}_1$  and  $\mathbf{s}_2$  were obtained by nonlinear programming [9].

Table 2: Estimated parameters

| Bands | s     | $k_1(m)$ | $k_2(m)$ | $\mathbf{s}_1$ | $\mathbf{s}_2$ | t     |
|-------|-------|----------|----------|----------------|----------------|-------|
| Band2 | 91.20 | 10       | -5       | 12.7           | 25.65          | 72.9  |
| Band3 | 142.9 | -1       | 8        | 11.92          | 25.6           | 108.7 |
| Band4 | 116   | -10      | -10      | 19.04          | 28.67          | 90    |

Table 3 shows the Effective Instantaneous Field of View (EIFOV) which is related to the standard deviation  $\mathbf{s}$  by the relation:  $\text{EIFOV}=2.66.\mathbf{s}$  [3].

Table 3: Eifov estimation

| Bands | $\mathbf{s}_1$ | $\mathbf{s}_2$ | Eifov <sub>1</sub> | Eifov <sub>2</sub> |
|-------|----------------|----------------|--------------------|--------------------|
| Band2 | 12.7           | 25.65          | 34                 | 68                 |
| Band3 | 11.92          | 25.6           | 32                 | 68                 |
| Band4 | 19.04          | 28.67          | 51                 | 76                 |

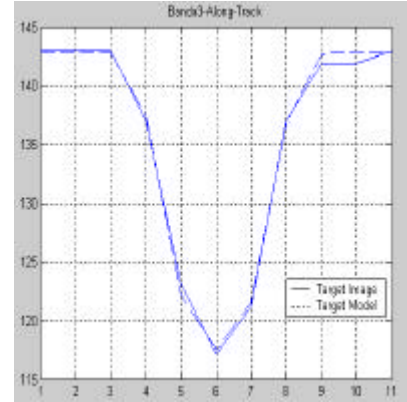


Figure 6. Band 3 along-track fitting

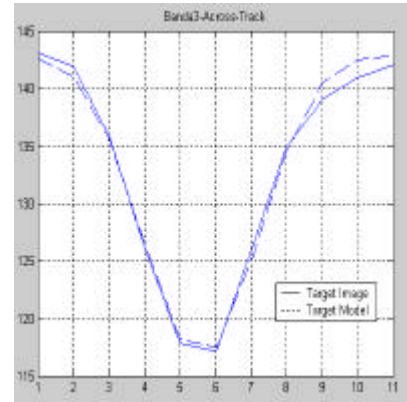


Figure 7. Band 3 across-track fitting

## 4. Conclusion

In this paper, an original approach of CBERS-1 CCD on-orbit PSF estimation has been introduced using images of a squared black target simulated on the Gobi desert. The results showed that CBERS-1 CCD across-track resolution is worst than the along-track one. In order to confirm these results other experiments are being performed with images of natural scenes such as images of Rio-Niteroi bridge in Rio de Janeiro and Portchain bridge in Lousiane.

## 5. References

- [1] Alves da Silva, E. "Cartography and remote sensing in the Amazon: the Sivam project". In: International Archives of Photogrammetry and Remote Sensing (IAPRS), 1998, Stuttgart, Germany. *Proceedings...* 1998. (v. 32).
- [2] Banon, G. J. F. *Formal introduction to digital image processing*. São José dos Campos: INPE, 2000. (INPE-7682-PUD/097). Posted in the URLib digital library: [dpi.inpe.br/banon/1999/06.21.09.31](http://dpi.inpe.br/banon/1999/06.21.09.31). Access in: 2003, Oct. 29.
- [3] Banon, G. J. F.; Santos, A. C. *Digital filter design for sensor simulation: application to the Brazilian Remote Sensing Satellite*. Sao Jose dos campos: INPE, 1993. 62 p. (INPE-5523-RPQ/665). Posted in the URLib digital library: [dpi.inpe.br/banon/1995/12.14.18.12](http://dpi.inpe.br/banon/1995/12.14.18.12). Access in: 2003, Oct. 29.
- [4] Banon, G. J. F.; Fonseca, L. M. G. *CBERS simulation from SPOT and its restoration*. CP 515, 12201-970 São José dos Campos, SP, Brazil: Instituto Nacional de Pesquisas Espaciais - INPE, 1998. Posted in the URLib digital library: [dpi.inpe.br/banon/1998/05.18.09.47](http://dpi.inpe.br/banon/1998/05.18.09.47). Access in: 2003, Oct. 29.
- [5] Bretschneider, T. "Blur identification in satellite imagery using image doublets". In: Asian Conference on Remote Sensing, 2002, Kathmandu, Nepal *Proceedings...* 2002.
- [6] Choi, T.; Helder, D. L. "Techniques for measuring the in-orbit modulation transfer function (MTF) for high spatial resolution imaging satellite". In: High Spatial Resolution Commercial Imagery Workshop, Mar. 2001, Greenbelt, USA. *Proceedings...* 2001.
- [7] Fonseca, L. M. G. *Determinação e avaliação das funções de transferência de modulação (MTF) dos sistemas MSS e TM (Landsat-5)*. São Jose dos Campos: INPE, 1987. 19 p. (INPE-4187-RPE/543).
- [8] Fonseca, L. M. G.; Mascarenhas, N. D. D. "Determinação da função de transferência do sensor TM do satélite Landsat-5". In: Congresso Nacional de Matemática Aplicada e Computacional, 10., 21-26 set. 1987, Gramado, BR. *Resumo dos Trabalhos...* 1987. p. 297-302. Publicado como: INPE-4213-PRE/1094.
- [9] Himmelblau, D. M. *Applied Nonlinear Programming*. New York: McGraw-Hill Book Company, 1972.
- [10] Kuga, H. K.; Orlando, V. "Orbit control of CBERS-1 satellite at INPE". In: 16th International Symposium on Space Flight Dynamics, 2001, Pasadena, USA. *Proceedings...* 2001.
- [11] Malaret, E. R. *Methods of image restoration for incoherent and coherent systems*. Dec.. PhD Thesis - Purdue University, West Lafayette, IN. 1985.
- [12] Souza, P. E. U. *Calibração radiométrica de câmara CCD/CBERS-1.* maio 2003. Dissertação (Mestrado em Sensoriamento Remoto) - Instituto Nacional de Pesquisas Espaciais, São José dos Campos. 2003.
- [13] Storey, J. C. "Landsat 7 on-orbit modulation transfer function estimation". In: Sensors, Systems, and Next Generation Satellites V, 17-20 Sep. 2001, Toulouse, France. *Proceedings...* Bellingham, WA, USA: SPIE, 2001. p. 50-61. (Proceedings of SPIE , v. 4540).
- [14] Wang, G.; Li, Y. "Axiomatic approach for quantification of image resolution". *IEEE Signal Processing Letters*, v. 6, p. 257-258, 1999.